Artificial selection for structural color on butterfly wings and comparison with natural evolution

Bethany R. Wasik[a,1], Seng Fatt Liew[b,1], David A. Lilien[b,1], April J. Dinwiddie[a], Heeso Noh[b,c], Hui Cao[b,2], and Antónia Monteiro[a,d,e,2]

[a]Department of Ecology and Evolutionary Biology, Yale University, New Haven, CT 06511; [b]Department of Applied Physics, Yale University, New Haven, CT 06511; [c]Department of Nano and Electronic Physics, Kookmin University, Seongbuk-Gu, Seoul 136-702, South Korea; [d]Department of Biological Sciences, National University of Singapore, Singapore 117543; and [e]Yale-NUS College, Singapore138614

Edited by David A. Weitz, Harvard University, Cambridge, MA, and approved June 28, 2014 (received for review February 13, 2014)

Brilliant animal colors often are produced from light interacting with intricate nano-morphologies present in biological materials such as butterfly wing scales. Surveys across widely divergent butterfly species have identified multiple mechanisms of structural color production; however, little is known about how these colors evolved. Here, we examine how closely related species and populations of *Bicyclus* butterflies have evolved violet structural color from brown-pigmented ancestors with UV structural color. We used artificial selection on a laboratory model butterfly, *B. anynana*, to evolve violet scales from UV brown scales and compared the mechanism of violet color production with that of two other *Bicyclus* species, *Bicyclus sambulos* and *Bicyclus medontias*, which have evolved violet/blue scales independently via natural selection. The UV reflectance peak of *B. anynana* brown scales shifted to violet over six generations of artificial selection (i.e., in less than 1 y) as the result of an increase in the thickness of the lower lamina in ground scales. Similar scale structures and the same mechanism for producing violet/blue structural colors were found in the other *Bicyclus* species. This work shows that populations harbor large amounts of standing genetic variation that can lead to rapid evolution of scales' structural color via slight modifications to the scales' physical dimensions.

thin film | constructive interference | parallel evolution | photonics

Organisms produce colors in two basic ways: by synthesizing pigments that selectively absorb light of certain spectral bands so that only light outside the absorption bands is backscattered (chemical color) or by developing nanomorphologies that enhance the reflection of light of certain wavelengths by interference (physical color or structural color). Structural colors play major roles in natural and sexual selection in many species (1) and have a broad range of applications in color display, paint, cosmetics, and textile industries (2). Structural color surveys across widely divergent species have revealed a large diversity of color-producing mechanisms (3–9). However, there has been a lack of systematic study and comparison of how different colors from closely related species or within populations of a single species evolve, even though these colors can vary dramatically. By examining how these species/populations evolve different colors, it is possible to identify the minimal amount of morphological change that results in significant color variation. Furthermore, this research may serve as an inspiration for future application of similar evolutionary principles to the design of photonic devices for color tuning, light trapping, or beam steering (2, 10–20). From an evolutionary biology point of view, we are curious to examine how structural colors respond to selection pressure and whether there is sufficient standing genetic variation in natural populations to allow the rapid evolution of novel colors. Here we focus on determining the morphological changes and the physical mechanisms that cause the evolution of violet structural color in populations of a single species and also across different species within a single genus of butterflies.

We focus on the genus *Bicyclus* (Lepidoptera: Nymphalidae), composed of more than 80 species that predominantly exhibit brown color along with marginal eyespots. Some *Bicyclus* species, however, have independently evolved transverse bands of bright violet/blue structural color on the dorsal surface of the forewings (black asterisks in Fig. 1*A*) (21, 22). One species, *Bicyclus anynana*, has become a model species amenable to laboratory rearing, and multiple aspects of its marginal eyespots (size, relative width of the color rings, shape) have been altered by artificial selection (23–27). However, change of color (hue), either pigmentary or structural, via artificial selection has not been reported. *B. anynana* does not exhibit bright violet coloration on its wings and therefore provides an excellent opportunity for investigating whether there is genetic potential to produce violet color upon directed selection. We investigated this potential by performing an artificial selection experiment in *B. anynana* that targeted the color of the specific dorsal wing region that evolved violet/blue coloration in other members of the genus (Fig. 1 *B–G*).

B. anynana, like other butterflies, has two types of scales, cover and ground, which alternate within a row with cover scales partially covering the ground scales and the point where both scales attach to the wing membrane (Fig. 1 *H* and *I* and Fig. S1) (28). Both cover and ground scales contain a lower lamina with a continuous smooth surface below a region composed of longitudinal ridges and crossribs, collectively referred to as the "upper lamina" and connected to the lower lamina via pillars

Significance

Despite significant efforts to study structural colors in nature, little is known about how such colors and structures evolved in the first place. To address this key question, we performed the first artificial selection (to our knowledge) on a structural color using butterflies. We demonstrated rapid evolution of violet structural color from ultra-violet brown scales in *Bicyclus anynana* butterflies with only six generations of selection. Furthermore, we identified the structural changes responsible for color evolution, which involve changes in the thickness of a chitin lamina in individual wing scales. By examining other violet-banded species that occur naturally in the *Bicyclus* genus, we found the colors are produced via the same mechanism and thus may have evolved via similar scale modifications.

Author contributions: H.C. and A.M. designed research; B.R.W., S.F.L., D.A.L., A.J.D., and H.N. performed research; B.R.W., S.F.L., D.A.L., H.N., H.C., and A.M. analyzed data; and B.R.W., S.F.L., H.C., and A.M. wrote the paper.

The authors declare no conflict of interest.

This article is a PNAS Direct Submission.

Freely available online through the PNAS open access option.

[1]B.R.W., S.F.L., and D.A.L. contributed equally to this work.

[2]To whom correspondence may be addressed. Email: hui.cao@yale.edu or antonia.monteiro@nus.edu.sg.

This article contains supporting information online at www.pnas.org/lookup/suppl/doi:10.1073/pnas.1402770111/-/DCSupplemental.

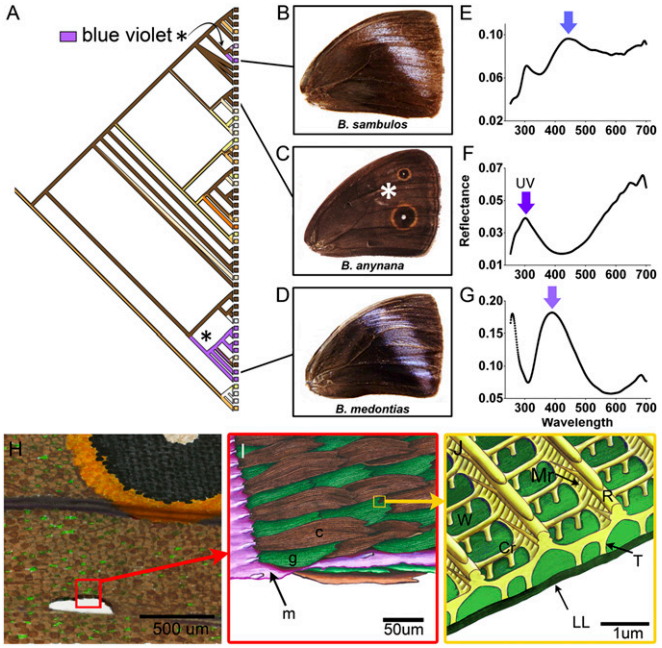

Fig. 1. Structural color in *Bicyclus* butterflies and basic wing scale morphology. (*A*) A phylogenetic estimate of *Bicyclus* butterfly relationships (modified from ref. 41) illustrating the evolution of color in the genus. The black asterisks mark two clades that evolved violet/blue color independently, represented here by *B. sambulos* and *B. medontias*. (*B–D*) Dorsal wing images of *B. sambulos*, *B. anynana* (the region used for artificial selection is marked by white asterisk), and *B. medontias*. (*E–G*) Graphs of reflectance spectra of the blue/violet wing band showing reflectance peaks in the 400–450 nm range and in the brown-colored homologous region in *B. anynana* with a UV reflectance peak centered at 300 nm (colored arrows). (*H*) 3D illustration of the wing and scales in the selected wing area of *B. anynana*. (*I*) Magnified view of the ripped region in *H* showing how cover (c; brown) and ground (g; green) scales are attached to the wing membrane (m, pink) and alternate along rows. Scales on the other (ventral) side of the wing membrane are visible also. (*J*) Cross-sectional view of a single scale showing the trabeculae (T) connecting the lower lamina (LL) to the upper lamina that includes ridges (R), microribs (Mr), and crossribs (Cr). Windows (W) are the spaces between the ridges and crossribs. Cover and ground scales have the same basic morphology. [Illustrations in *H–J* courtesy of Katerina Evangelou (Central Saint Martin's College, London).]

called "trabeculae" (Fig. 1*J* and Fig. S1) (6). Previous studies on butterflies showed that structural color can be produced by interference with light reflected from the overlapping lamella that build the longitudinal ridges, from microribs protruding from the sides of the longitudinal ridges, or from the lower lamina, which can vary in thickness and patterning (Fig. 1*J*) (29, 30). However, it is not clear how the violet/blue color is produced in members of the two *Bicyclus* clades that separately evolved this color, whether *B. anynana* can be made to evolve the same violet/blue color via artificial selection, and whether it will generate the color in the same way as the other species. To answer these questions, we conducted detailed optical characterization and structural analysis of butterfly wing scales from three separate species and artificially evolved populations of *Bicyclus* to illustrate how color is generated and how it has evolved.

Results

Artificial Selection for Violet Scale Color in *B. anynana*. Optical reflectance spectra of the violet/blue-colored bands on the dorsal forewings of two representative species from the two clades that independently evolved violet/blue color, *Bicyclus sambulos* and *Bicyclus medontias,* exhibit peaks in the wavelength range of 400–450 nm (Fig. 1 *E* and *G*). The reflectance spectrum from the same wing region in *B. anynana* does not show any peak in the violet/blue wavelength range (~380–495 nm) but does show a peak in the UV range at the wavelength of 300 nm (Fig. 1*F*). The aim of our artificial selection experiment was to shift this UV peak to the violet/blue range of the spectrum.

We artificially selected the most extreme *B. anynana* individuals of each sex by measuring their reflectance spectra from a region of the dorsal forewing associated with violet/blue color in other *Bicyclus* species (white asterisk in Fig. 1*C*). Individuals displaying reflectance peaks nearest to 400 nm were bred with each other, and this procedure was repeated six times during eight consecutive generations. (Because of low adult numbers, all individuals in generations 4 and 7 were allowed to reproduce and did not undergo selection.) This procedure led to a gradual increase in the reflectance peak wavelength for the selected population. In the parental generation (generation 1), the average wavelength of the reflectance peak for the targeted dorsal region was 311 nm for males and 341 nm for females. By generation 8, the peaks had shifted to 362 nm and 385 nm in males and females, respectively (Fig. 2*A*). Selected individuals exhibited significantly increased reflectance in the wavelength range of 400–500 nm (Table S1).

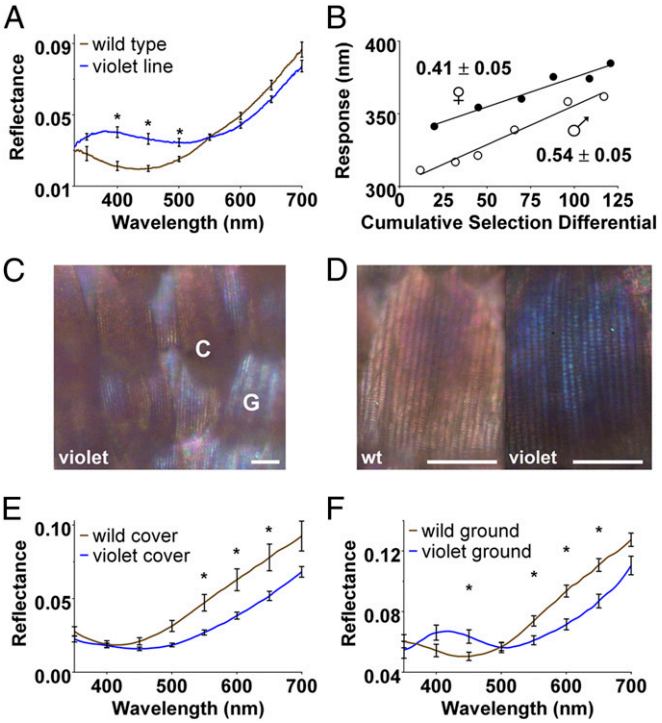

Fig. 2. Artificial selection of violet structural color in *B. anynana*. (*A*) Representative reflectance spectra of WT and violet-line females. (*B*) Response to selection plotted against a cumulative measure of the selection pressure applied to each generation and realized heritability estimates for reflectance peak wavelength in *B. anynana* females (filled circles) and males (open circles) over six generations of selection (*Materials and Methods*). (*C*) Image of violet-line cover (C) and ground (G) scales with the violet hue visible only in ground scales. (*D*) Images of WT (*Left*) and violet-line (*Right*) ground scales (generation 8) in the selected wing region. (Scale bars in *C* and *D*: 20 μm.) (*E* and *F*) Mean reflectance spectra of five WT and five violet-line females for cover scales (*E*) and for ground scales on the wing with cover scales removed (*F*). In all graphs, error bars represent SEM, and asterisks represent statistically significant differences in reflectance (Table S1). Note that the reflectance from ground scales with cover scales removed in *F* peaked at a slightly longer wavelength than the reflectance taken directly from an intact violet-line wing in *A* because *A* included both ground scales and cover scales averaged over a relatively large area.

The proportion of the variation in reflectance peak wavelength displayed by individuals in the laboratory population that is caused by additive genetic variation, as opposed to environmental or other types of genetic variation, is around 50% [e.g., the realized heritabilities are 0.41 (41%) in females and 0.54 (54%) in males] (Fig. 2*B*), hence the rapid response to selection. This measure of heritability was estimated from the selection pressure applied and the response to selection (reflectance peak wavelength shift) (*Materials and Methods*). In summary, our artificial selection experiment demonstrated that *B. anynana* laboratory populations have significant additive genetic variation controlling reflectance peak wavelength that allowed the rapid evolution of a novel scale color.

Changes in Ground Scales Led to Evolution of Violet Color in *B. anynana*. To determine how the violet color evolved, we performed optical measurements on the wings of females from generation 8 whose dorsal reflectance peak was closest to 400 nm (Fig. 2*A*). Comparisons of optical images of WT and violet-line *B. anynana* female wings revealed patches of violet color in the violet-line individuals from regions where cover scales were missing and ground scales were fully exposed, suggesting that the violet color is produced by the ground scales (Fig. 2*C*). Indeed, high-magnification images of single ground scales from violet-line females showed an intense violet reflection compared with scales from WT females (Fig. 2*D*). To investigate in a quantitative manner which scale types primarily contributed to the violet color, we measured reflectance spectra from individual cover scales (while attached to the wing) from both WT and violet-line females, from ground scales after some cover scales were removed, and finally from the wing membrane with both cover and ground scales removed.

We found no significant changes in the violet reflectance of cover scales or wing membranes between WT and violet-line individuals (Fig. 2*E*, Fig. S2, and Table S1). However, ground scales in violet-line females exhibited a significant increase in reflectance between 400 nm and 450 nm compared with WT ground scales (Fig. 2*F* and Table S1). We conclude that changes to the ground scales in *B. anynana* are primarily responsible for the evolution of violet color in this artificial selection experiment.

To pinpoint where the violet color was produced, we isolated single cover and ground scales and measured reflectance spectra from both the abwing and adwing scale surfaces (i.e., the surfaces facing away from and toward the wing membrane, respectively). Our results confirmed that violet-line ground scales exhibited more visible violet color (matching the reflectance spectra) than WT ground scales (Fig. 3 *A* and *B*). Both surfaces of the violet-line scales, but especially the adwing surface, had significantly higher reflectance in the violet range of the spectrum (380–450 nm) than the corresponding surface of WT ground scales (Table S1). The higher reflectance from the adwing surface of the violet-line ground scales indicates that the violet color originates from the lower lamina of the scale. The adwing of cover scales also showed a significant increase in reflectance at the violet wavelength (~450 nm), but the abwing reflectance barely changed (Fig. S3 and Table S1). Therefore, both ground and cover scales evolved violet color, which is produced in the lower lamina of the scales, but ground scales changed more dramatically.

To explore whether changes in scale pigmentation contributed to the evolution of scale color and to understand the difference in reflectance from the adwing and abwing surfaces, we measured light transmission through isolated cover and ground scales and obtained the absorbance spectra from the measured transmittance of scales immersed in fluid matching the refractive index. The violet-line ground scales exhibit significantly higher transmission or lower absorption than their WT counterparts (Fig. 3 *C* and *D* and Table S1). Variation in transmission is caused by light absorption by pigments observed in the mass of the scales. The reduced absorption in the violet-line scales increases the reflection of light from the lower lamina of these scales. In addition, the ridges and crossribs were less transmissive areas across all scale types, and these structures appear to have evolved a thinner appearance in violet-line scales than in WT scales (Fig. S4). These changes in morphology on the upper surface of the scale contribute to the lower absorption of the violet-line scales. Differences in reflectance measured from adwing and abwing surfaces can be attributed to additional absorption and scattering of light by the ridges and cross-ribs that are present only in the upper lamina (Fig. 3*C*) (30). Hence, the appearance of the violet color resulted from a combination of enhanced reflection and reduced absorption by the violet-line ground scales.

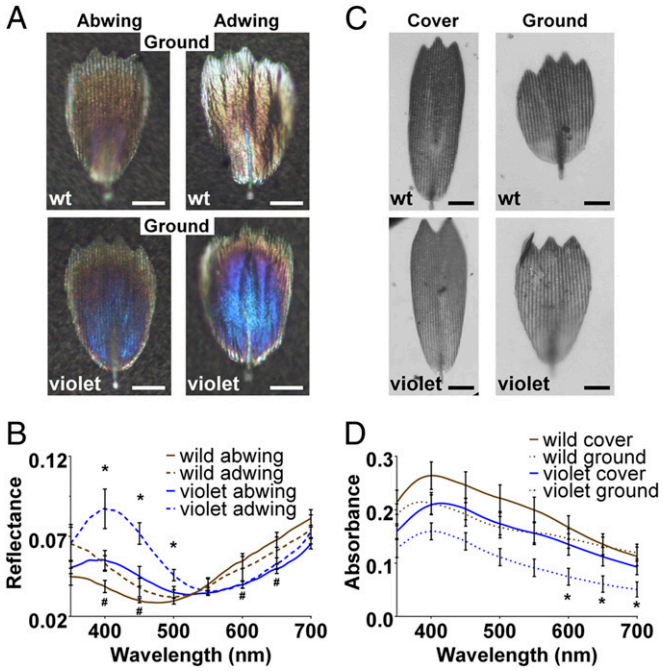

Fig. 3. Evolution of violet color in *B. anynana* ground scales. (*A*) Images of abwing (*Left*) and adwing (*Right*) surfaces of individual ground scales from WT (*Upper Row*) and violet-line (*Lower Row*) females. (*B*) Reflectance spectra of individual ground scales from WT and violet-line individuals. (*C*) Transmission images for *B. anynana* WT (*Upper Row*) and violet-line (*Lower Row*) cover scales (*Left*) and ground scales (*Right*). (Scale bars in *A* and *C*: 20 μm.) (*D*) Absorbance measurements for individual scales. In *B* and *D*, error bars represent SEM. Asterisks indicate statistically significant differences in reflectance or absorbance between lines for the adwing scale surfaces (*B*) or ground scales (*D*), respectively; pound symbols (#) indicate statistically significant differences in reflectance for the abwing scale surfaces (*B*) (Table S1).

Structural Analysis of Violet Scales. To discover the mechanism that produces the violet color in selected *B. anynana*, we collected scanning electron microscope images of the scale's nanomorphologies. Although cover scales are more elongated than ground scales, their nanomorphologies are similar, i.e., both have a typical ridge–lamellar structure similar to previously described nymphalid wing scales (28, 29) (Fig. 1*J*). Note also that the lower lamina is clearly visible through the windows in the upper lamina (Fig. S4). A direct comparison of optical and scanning electron microscope images of the same cross-sectioned scales allowed us to measure the thickness of the lower lamina from the color-producing region of cover and ground scales (Fig. 4 *A* and *B*). Using measurements from multiple scales, we were able to estimate the average lamina thickness for each scale type (Fig. 4*C*). Although unselected *B. anynana* cover and ground scale lower laminae have almost the same thickness (~120 nm), both became

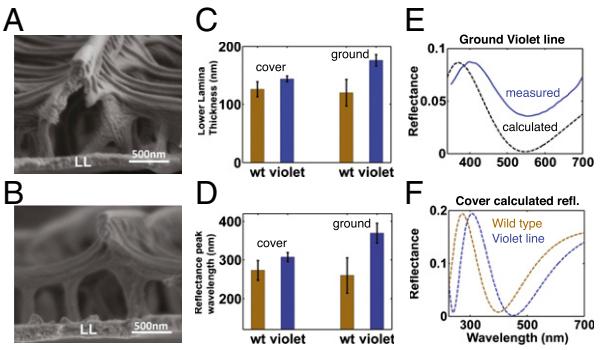

Fig. 4. Scanning electron micrographs of *B. anynana* scales and calculated reflectance spectra. (*A* and *B*) Magnified cross-sectional scanning electron micrograph images of lower lamina (LL) in a WT cover scale (*A*) and a violet-line ground scale (*B*). (*C*) Mean lower lamina thickness measured from the cross-sectional scanning electron micrograph images of cover and ground scales of WT and violet-line *B. anynana*. The error bars represent 95% confidence intervals for the means. (*D*) Calculated reflectance peak wavelengths of lower lamina using the individually measured thickness values of cover and ground scales of WT and violet-line *B. anynana*. (*E*) Comparison of the calculated (dashed line) and measured (solid line) reflectance spectra of the violet-line ground scales. Because our calculations did not include absorption caused by pigments in the thin film, the magnitude of the calculated reflectance peak is higher than that of the measured peak. Peak magnitudes were normalized by lowering the magnitude of the calculated reflectance peak to match the magnitude of the measured peak. (*F*) Calculated reflectance spectra for the cover scales of WT (brown dashed line) and violet-line (purple dashed line) *B. anynana*.

thicker through artificial selection. The thickness of cover scale lamina increased from 126 ± 13 nm (95% confidence interval) to 144 ± 5 nm ($F = 2.8$, $P = 0.142$), whereas the thickness of ground scales increased significantly, from 120 ± 23 nm in WT to 176 ± 10 nm in the violet-line individuals ($F = 21.8$, $P < 0.01$).

To investigate whether the increases in lower lamina thickness were responsible for the spectral shifts in reflectance peaks (i.e., in scale color), we numerically calculated the reflectance spectra for the lower lamina by modeling it as a dielectric thin film. Lamina thickness was set to the measured values for each scale type, and the refractive index and its variation with wavelength were set according to previous measurements of nonpigmented chitin from butterfly wing scales (31). We also took into account the range of incident angle of the light and the variation in the thickness of the lower lamina (*Materials and Methods*). However, we did not include lamina absorption caused by pigments in the calculation, because it is not known how much of the measured absorbance occurred in the lower versus upper lamina. In the violet-line ground scales, the measured and calculated reflectance spectra exhibited similar modulation with wavelength, giving a clear spectral signature confirming that the reflectance peak is produced by thin-film interference (Fig. 4*E*). However, the calculated peak wavelength (374 nm) is slightly lower than the average measured peak wavelength (405 nm) (Fig. 4*E*). Similar results were obtained for the WT ground scales. In sum, the calculated spectral shift from WT to violet-line ground scales is close to the measured shift, but the calculated reflectance peaks have a shorter wavelength (Fig. 4*D*). For the cover scales, the calculated shift in reflectance peaks was from 273 nm (WT) to 310 nm (violet-line) (Fig. 4*F*). These calculated reflectance peak wavelengths also were slightly lower than the measured values (~300 nm in Fig. 1*F*). The peak remained in the UV range because the increment of lower lamina thickness was smaller in cover scales than in ground scales. Simultaneously, the calculated reflectance at longer wavelengths (500–700 nm) was reduced (Fig. 4*F*), in agreement with results in Fig. 2*E*. Consequently, the violet-line cover scales appeared dark violet compared with the WT cover scales (Fig. S3*B*).

We attribute these discrepancies in the simulated and measured reflectance peak wavelengths to a modification of the refractive index of the lower lamina induced by pigments within it; this modification was not included in our calculation. The measured absorbance spectra of our various scale types (Fig. 3*D*) do not match the melanin absorbance spectrum exactly (30, 32, 33), indicating that brown scales in *B. anynana* either do not contain melanin or, more likely, contain additional pigments besides melanin. Because the type and amount of pigments that exist in the lower lamina of scales are not known, we cannot accurately estimate the change of refractive index value caused by pigmentation. However, the shape of the measured reflectance spectra and the direction of the observed spectral shifts of the reflectance peak from UV to violet indicate that the observed color change in ground scales is caused by the increased thickness of the lower lamina of these scales.

Natural Evolution of Violet/Blue Color Within the *Bicyclus* Genus. After demonstrating that *B. anynana* can readily produce violet colored scales, we investigated how the other members of the *Bicyclus* genus naturally evolved their violet/blue colors. The *Bicyclus* genus is composed of more than 80 species (21, 22), and violet/blue color has evolved independently twice in two separate lineages (black asterisks in Fig. 1*A*). To identify the primary sources of violet/blue color on the dorsal wing bands of these species, we isolated cover and ground scales from representative species from each lineage, *B. sambulos* and *B. medontias* (Fig. 1 *B* and *D*), and examined their reflectance and transmittance spectra.

In *B. sambulos*, optical reflectance images of isolated cover and ground scales revealed that the violet/blue color came predominantly from the cover scales (Fig. 5*A*). Reflectance measurements showed enhanced light reflection in the wavelength range of 400–500 nm from both sides of the cover scale, whereas

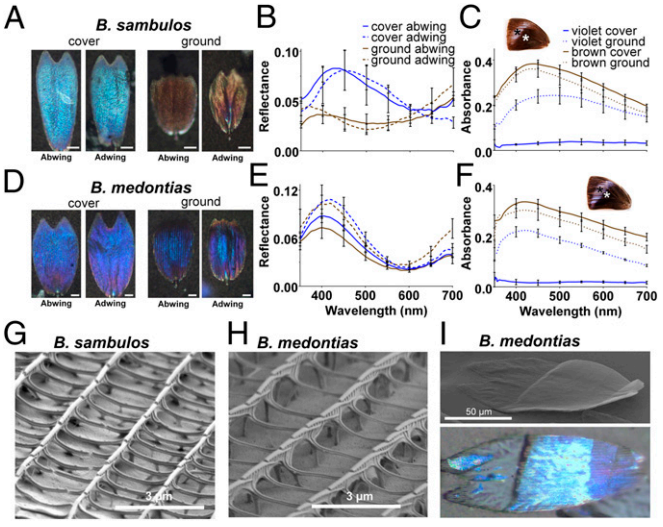

Fig. 5. Violet/blue structural color in *B. sambulos* and *B. medontias*. (*A*) Images of abwing and adwing surfaces of individual cover (*Left*) and ground (*Right*) scales from *B. sambulos*. (*B*) Reflectance spectra of individual cover and ground scales. (*C*) Absorbance measurements for *B. sambulos* scales from the violet/blue region (black asterisk in *Inset*) and the brown region of the dorsal wing (white asterisk in *Inset*). (*D–F*) As above but for scales from *B. medontias*. (Scale bars in *A* and *D*: 20 µm.) Error bars in *B*, *C*, *E*, and *F* represent SEM. (*G*) Scanning electron microscope image of a *B. sambulos* cover scale, showing nanomorphology similar to that of *B. anynana* (Fig. S1). (*H*) Scanning electron microscope image of a *B. medontias* cover scale, also showing nanomorphology similar to that of *B. anynana*. (*I*) Scanning electron microscope (*Upper*) and optical image (*Lower*) showing part of a *B. medontias* scale (with adwing surface facing up) adhering to the substrate, leading to the disappearance of color produced by thin-film interference.

ground scales had no peak in this wavelength range (Fig. 5*B*). Absorbance measurements (Fig. 5*C*) and transmission images (Fig. S5*A*) show that cover scales from the violet/blue dorsal band region had the lowest absorbance, followed by ground scales in the same region, compared with the cover and ground scales in the adjacent brown region. Because the cover scales in the violet/blue wing band region of *B. sambulos* were much less pigmented than those of *B. anynana*, the difference in reflectance measured from both abwing and adwing surfaces is much smaller. Scanning electron microscope images of *B. sambulos* cover and ground scales (Fig. 5*G* and Fig. S4) revealed nanomorphologies similar to those in the scales of *B. anynana*. From the cross-sectional scanning electron microscope images, we measured the lower lamina thickness of cover scales to be 204 ± 13 nm. These measurements produce a calculated reflectance spectrum with a peak at 428 ± 26 nm, which agrees well to the measured reflectance peak at 450 nm (Fig. 5*B*). These results confirm that the violet/blue color is produced via thin-film interference in the lower lamina of cover scales. In summary, the violet/blue color of *B. sambulos* is produced primarily by cover scales, not by ground scales as we observed in *B. anynana*, but the mechanism of color production is the same in both species.

In *B. medontias*, the violet color was visible from both sides of cover and ground scales (Fig. 5*D*). The scales' optical reflectance data (Fig. 5*E*) were similar to the reflectance data of *B. sambulos* cover scales, except for a slight shift in the wavelengths of the reflectance peaks. The scales' absorbance data (Fig. 5*F*) also were similar to those of *B. sambulos*, where the violet scales had lower absorption than the adjacent brown scales. Scanning electron microscope images of the violet scales (Fig. 5*H* and Fig. S4) showed scale nanomorphologies similar to those of both *B. anynana* and *B. sambulos*, suggesting that the violet color is produced by the same mechanism. Thin-film interference was confirmed further by the disappearance of the violet color in a part of a cover scale of *B. medontias* that adhered to the substrate (Fig. 5*I*). Color produced by thin-film interference relies on the interference of light reflected from the top and bottom surfaces of a thin film, such as the lower lamina of a scale. When one side of the scale lamina is attached to the closely index-matched substrate, light reflection from that interface is greatly reduced; thus the thin-film interference diminishes, and color disappears, as observed in Fig. 5*I*.

Discussion

Here we document the first (to our knowledge) study in butterflies of the evolution of structural color by artificial selection and show that structural violet color can evolve in a short period (six generations) in a laboratory-reared butterfly population. We also show that violet/blue structural color has evolved independently within a genus and that the descendant species use the same mechanism for color generation (thin-film interference) but in different scale types: ground scales in *B. anynana*, cover scales in *B. sambulos*, and both scale types in *B. medontias*. Violet structural color in *B. anynana* evolved via changes in cuticular properties (i.e., thickness) of the lower lamina of individual wing scales, concurrently with a decrease in absorption in the same scales.

Structural color is produced more often by cover scales because they overlay ground scales and are more exposed to incident light (6). Thus, the evolution of violet color in *B. anynana* ground scales is unexpected, and we speculate it may be a result of the artificial selection procedure. The relatively high-density cages where we kept the animals before they were measured and selected and the handling during measurement may have led to partial loss of some cover scales, preferentially exposing the ground scales to selection and leading to their more extensive modification. This unexpected result, compared with the natural evolution of blue color in the other species of *Bicyclus*, revealed that both cover and ground scales in *B. anynana* have the remarkable potential to be modified independently through the process of selection.

Our results, in conjunction with other recent studies (34), suggest that structural colors can evolve rapidly and ultimately play pivotal roles in butterfly fitness and diversity. For instance, structurally colored wing patterns in butterflies have been proposed to function as species recognition signals, as sexually dimorphic signals involved in female mate choice, and as signals that are predictive of nuptial gift size (34–37). Furthermore, the evolution of these colors in only certain species of a genus, as we have documented here for *Bicyclus*, may depend less on the availability of genetic variation in natural populations for producing these colors and more on natural or sexual selection favoring specific colors. Although we know of no comparable artificial selection study on pigmentary color in butterflies, previous research on pigmentary color evolution in birds revealed that shifts to new diets and/or gains/losses of enzymatic steps in biochemical pathways were required to modify the color resulting from pigments acquired through diet (38, 39). In contrast, structural colors, as exemplified here, can evolve simply via quantitative variation in the amount of cuticular secretions produced by individual cells, without the modification of any additional material property. Therefore in nature structural colors may evolve more rapidly than pigmentary colors; this possibility should be examined in the future.

Finally, by identifying a process, artificial selection, that can lead readily to structural color evolution in butterflies, our study lays the ground for future research on the genetics of structural colors, e.g., by crossing selected lines within a species, followed by linkage mapping. In addition, the artificial selection used in this study may inspire future applications of similar evolutionary principles to the design of reconfigurable photonic materials and devices.

Materials and Methods

Experimental Animals. *B. anynana* were reared at 27 °C, 80% humidity, as previously described (40). Upon eclosion, virgin male and female adults were isolated from one another to ensure virginity and were kept in cooler conditions (17 °C) until all animals of that generation emerged and were measured. Selected adults were mated with each other and subsequently were preserved in glassine envelopes and stored at −20 °C. Scanning electron microscope and reflection microspectrophotometry analyses were done with females of *B. anynana* and male specimens of two other species: *B. sambulos*, collected in September 2012 from the Lake Kivu region of the eastern Democratic Republic of Congo, and *B. medontias*, collected from the Ebogo region of Cameroon, both generously provided by Steve Collins (African Butterfly Research Institute, Nairobi, Kenya). A multilocus phylogenetic estimate of *Bicyclus* relationships was constructed and modified from previous *Bicyclus* studies to illustrate the relationship between *B. anynana*, *B. sambulos*, and *B. medontias* (41). Briefly, this estimate is the consensus of trees drawn from a posterior distribution populated by a Metropolis-coupled Markov chain Monte Carlo exploration of tree likelihood space (42).

Selection Procedure. For each generation, scale reflectance was measured in a prespecified region of the dorsal forewing (~1 mm in diameter; white asterisk in Fig. 1*C*) using a spectrophotometer (Ocean Optics 2000) and the accompanying program, SpectraSuite (Ocean Optics). Each individual was measured in triplicate and numbered on the hindwing. Reflectance values of individuals were analyzed using a selection script in MATLAB (v. 2011a; MathWorks, Inc.). Individuals exhibiting reflectance peak wavelengths in the UV range that were most shifted toward the 400-nm wavelength were selected as breeders for the next generation. We reared eight generations of animals. Selection intensity varied from generation to generation, but ~15–30 individuals were selected per sex in each generation. In generations 4 and 7, no selection was applied because of the small populations of emerged adults; all individuals were mated together to produce generations 5 and 8.

Realized Heritability. The proportion of the variation in reflectance peak wavelength that is caused by additive genetic variation in our laboratory population is called the "realized heritability" (43). This measure of heritability was estimated from two quantities: the response to selection and the cumulative selection differential. The response to selection (*y* axis in Fig. 2*B*) tracks the change in mean reflectance peak wavelength for all individuals in a generation over the course of the selection experiment. The cumulative selection differential (*x* axis in Fig. 2*B*) is a cumulative measure of the selection pressure applied in

each generation. The selection pressure applied in a particular generation is estimated by subtracting the mean reflectance peak wavelength of all individuals in a generation from the mean reflectance peak wavelength of the selected individuals in that generation. In Fig. 2*B* the response of one generation is plotted against the cumulative selection differential of the previous generations. From a linear fit of the data, we obtained the slope, which is the realized heritability. Graphs for realized heritability and reflectance data were constructed using GraphPad Prism (v. 6.00; GraphPad Software).

Scale Imaging and Microspectrophotometry. Details are given in *SI Materials and Methods*.

Scanning Electron Microscopy. Details are given in *SI Materials and Methods*.

Numerical Simulations of Reflectance Spectra from Lower Lamina. A standard thin-film interference model considering multiple reflections within a dielectric film was used to calculate reflectance spectra from the lower lamina of wing scales (2). Details are given in *SI Materials and Methods*.

ACKNOWLEDGMENTS. We thank Katerina Evangelou for producing 3D hand-drawn illustrations of wing scales; Robert Rak and Chris Bolick for rearing corn plants for *B. anynana* larvae; Steve Collins at the African Butterfly Research Institute, Nairobi, Kenya, for providing specimens of *B. sambulos* and *B. medontias*; Kendra Robertson and Jeffrey Oliver for constructing the character state phylogeny; Morven Graham and Rose Webb for assisting with transmission electron microscopy imaging; Mohan Srinivasarao for supporting early versions of this project; Richard Prum for providing initial spectral data for *Bicyclus* species; Eric Dufresne for constructive discussions; and two reviewers for improving the quality of the paper. Use of the scanning electron microscope facility was supported by the Yale Institute for Nanoscience and Quantum Engineering and by National Science Foundation Grant MRSEC DMR-1119826. Funding was provided by National Science Foundation Grant PHY 0957680 (to A.M. and H.C.), the Ministry of Education Grant R-154-000-602-112 (to A.M.), and the Guggenheim Fellowship (to H.C.).

1. Shawkey MD, Morehouse NI, Vukusic P (2009) A protean palette: Colour materials and mixing in birds and butterflies. *J R Soc Interface* 6(Suppl 2):S221–S231.
2. Kinoshita S, Yoshioka S, Miyazaki J (2008) Physics of structural colors. *Rep Prog Phys* 71(7):1–30.
3. Eliason CM, Bitton PP, Shawkey MD (2013) How hollow melanosomes affect iridescent colour production in birds. *Proc Biol Sci* 280(1767):20131505.
4. D'Alba L, et al. (2011) Colour-producing β-keratin nanofibres in blue penguin (*Eudyptula minor*) feathers. *Biol Lett* 7(4):543–546.
5. Saranathan V, et al. (2012) Structure and optical function of amorphous photonic nanostructures from avian feather barbs: A comparative small angle X-ray scattering (SAXS) analysis of 230 bird species. *J R Soc Interface* 9(75):2563–2580.
6. Ghiradella H (1985) Structure and development of iridescent lepidopteran scales - The papilionidae as a showcase family. *Ann Entomol Soc Am* 78(2):252–264.
7. Wickham S, Large MC, Poladian L, Jermiin LS (2006) Exaggeration and suppression of iridescence: The evolution of two-dimensional butterfly structural colours. *J R Soc Interface* 3(6):99–108.
8. Seago AE, Brady P, Vigneron JP, Schultz TD (2009) Gold bugs and beyond: A review of iridescence and structural colour mechanisms in beetles (Coleoptera). *J R Soc Interface* 6(Suppl 2):S165–S184.
9. Vukusic P, Sambles JR (2003) Photonic structures in biology. *Nature* 424(6950): 852–855.
10. Gaillot DP, et al. (2008) Composite organic-inorganic butterfly scales: Production of photonic structures with atomic layer deposition. *Phys Rev E Stat Nonlin Soft Matter Phys* 78(3 Pt 1):031922.
11. Chung K, et al. (2012) Flexible, angle-independent, structural color reflectors inspired by morpho butterfly wings. *Adv Mater* 24(18):2375–2379.
12. Song F, Su H, Chen J, Zhang D, Moon W (2011) Bioinspired ultraviolet reflective photonic structures derived from butterfly wings (*Euploea*). *Appl Phys Lett* 99(16): 163705–163705-3.
13. Galusha JW, Jorgensen MR, Bartl MH (2010) Diamond-structured titania photonic-bandgap crystals from biological templates. *Adv Mater* 22(1):107–110.
14. Crne M, et al. (2011) Biomimicry of optical microstructures of *Papilio palinurus*. *Europhys Lett* 93(1):14001.
15. Harun-Ur-Rashid M, et al. (2010) Angle-independent structural color in colloidal amorphous arrays. *ChemPhysChem* 11(3):579–583.
16. Watanabe K, et al. (2005) Optical measurement and fabrication from a *Morpho*-butterfly-scale quasistructure by focused ion beam chemical vapor deposition. *J Vac Sci Technol B* 23(2):570–574.
17. Lee I, et al. (2010) Quasi-amorphous colloidal structures for electrically tunable full-color photonic pixels with angle-independency. *Adv Mater* 22(44):4973–4977.
18. Takeoka Y, Honda M, Seki T, Ishii M, Nakamura H (2009) Structural colored liquid membrane without angle dependence. *ACS Appl Mater Interfaces* 1(5):982–986.
19. Kumano N, et al. (2011) Multicolor polymer-dispersed liquid crystal. *Adv Mater* 23(7): 884–888.
20. Kumano N, Seki T, Ishii M, Nakamura H, Takeoka Y (2011) Tunable angle-independent structural color from a phase-separated porous gel. *Angew Chem Int Ed Engl* 50(17): 4012–4015.
21. Condamin M (1973) Monographie du genre *Bicyclus*: Lepidoptera Satyridae. PhD thesis (l'Institut Fondamental d'Afrique Noire, Dakar).
22. Monteiro A, Pierce NE (2001) Phylogeny of *Bicyclus* (Lepidoptera: Nymphalidae) inferred from *COI, COII*, and *EF-1alpha* gene sequences. *Mol Phylogenet Evol* 18(2): 264–281.
23. Monteiro A, Brakefield P, French V (1994) The evolutionary genetics and developmental basis of wing pattern variation in the butterfly *Bicyclus anynana*. *Evolution* 48(4):1147–1157.
24. Monteiro A, Brakefield P, French V (1997) Butterfly eyespots: The genetics and development of the color rings. *Evolution* 51(4):1207–1216.
25. Monteiro A, Brakefield PM, French V (1997) The genetics and development of an eyespot pattern in the butterfly *Bicyclus anynana*: Response to selection for eyespot shape. *Genetics* 146(1):287–294.
26. Beldade P, Brakefield PM, Long AD (2002) Contribution of *Distal-less* to quantitative variation in butterfly eyespots. *Nature* 415(6869):315–318.
27. Allen CE, Beldade P, Zwaan BJ, Brakefield PM (2008) Differences in the selection response of serially repeated color pattern characters: Standing variation, development, and evolution. *BMC Evol Biol* 8(94):94.
28. Nijhout HF (1991) *The Development and Evolution of Butterfly Wing Patterns* (Smithsonian Institution Press, Washington, D.C.).
29. Ghiradella H (1984) Structure of iridescent lepidopteran scales - variations on several themes. *Ann Entomol Soc Am* 77(6):637–645.
30. Stavenga DG, Leertouwer HL, Wilts BD (2014) Coloration principles of nymphaline butterflies - thin films, melanin, ommochromes and wing scale stacking. *J Exp Biol* 217(Pt 12):2171–2180.
31. Leertouwer HL, Wilts BD, Stavenga DG (2011) Refractive index and dispersion of butterfly chitin and bird keratin measured by polarizing interference microscopy. *Opt Express* 19(24):24061–24066.
32. Stavenga DG, Leertouwer HL, Hariyama T, De Raedt HA, Wilts BD (2012) Sexual dichromatism of the damselfly *Calopteryx japonica* caused by a melanin-chitin multilayer in the male wing veins. *PLoS ONE* 7(11):e49743.
33. Stavenga DG, Leertouwer HL, Wilts BD (2013) Quantifying the refractive index dispersion of a pigmented biological tissue using Jamin-Lebedeff interference microscopy. *Light Sci Appl* 2:e100.
34. Rajyaguru PK, Pegram KV, Kingston AC, Rutowski RL (2013) Male wing color properties predict the size of nuptial gifts given during mating in the Pipevine Swallowtail butterfly (*Battus philenor*). *Naturwissenschaften* 100(6):507–513.
35. Rutowski RL, Macedonia JM, Kemp DJ, Taylor-Taft L (2007) Diversity in structural ultraviolet coloration among female sulphur butterflies (Coliadinae, Pieridae). *Arthropod Struct Dev* 36(3):280–290.
36. Bálint Z, Kertész K, Piszter G, Vértesy Z, Biró LP (2012) The well-tuned blues: The role of structural colours as optical signals in the species recognition of a local butterfly fauna (Lepidoptera: Lycaenidae: Polyommatinae). *J R Soc Interface* 9(73):1745–1756.
37. Robertson KA, Monteiro A (2005) Female *Bicyclus anynana* butterflies choose males on the basis of their dorsal UV-reflective eyespot pupils. *Proc Biol Sci* 272(1572): 1541–1546.
38. McGraw KJ, Hill GE, Stradi R, Parker RS (2001) The influence of carotenoid acquisition and utilization on the maintenance of species-typical plumage pigmentation in male American goldfinches (*Carduelis tristis*) and northern cardinals (*Cardinalis cardinalis*). *Physiol Biochem Zool* 74(6):843–852.
39. Prum RO, LaFountain AM, Berro J, Stoddard MC, Frank HA (2012) Molecular diversity, metabolic transformation, and evolution of carotenoid feather pigments in cotingas (Aves: Cotingidae). *J Comp Physiol B* 182(8):1095–1116.
40. Westerman EL, Hodgins-Davis A, Dinwiddie A, Monteiro A (2012) Biased learning affects mate choice in a butterfly. *Proc Natl Acad Sci USA* 109(27):10948–10953.
41. Oliver JC, Monteiro A (2011) On the origins of sexual dimorphism in butterflies. *Proc Biol Sci* 278(1714):1981–1988.
42. Ronquist F, Huelsenbeck JP (2003) MrBayes 3: Bayesian phylogenetic inference under mixed models. *Bioinformatics* 19(12):1572–1574.
43. Falconer DS (1989) *Introduction to Quantitative Genetics* (Longman Wiley, Harlow, UK), 3rd Ed.

Supporting Information

Wasik et al. 10.1073/pnas.1402770111

SI Materials and Methods

Scale Imaging and Microspectrophotometry. All scale images were taken on a Nikon Optiphot 66 microscope in reflectance or transmission mode using BD Plan 5× to 40× lenses and a Moticam 2500 USB camera at maximum (5-megapixel) resolution. For the visible spectra the reflectance spectra were taken using an Ocean Optics HR2000+ spectrometer attached to the Nikon microscope. For the UV spectra the reflectance spectra were taken using a home-built microscope including an Oriel Instruments 66902 Xenon Arc Lamp and a Nikon TU Plan Fluor Epi 50× objective lens (numerical aperture = 0.8). Light emitted from the arc lamp was collected and directed toward the back aperture of the objective lens through two triplet lenses (aberration corrected from UV to near IR). To avoid tight focusing of light on the sample, the incident light filled only a central circular region of the back aperture (with a radius ∼20% of the back aperture radius). The range of incident angles of light was 15°. A variable aperture, located at a plane conjugated with the sample plane, was used to control the size of the illumination spot on the scales. In the single-scale measurements, the reflectance spectra were taken from the central lower region of isolated scales, and the illumination spot was 50 μm in diameter. Measurements performed on the wing were taken from three scales and/or wing areas from each of five different individuals, and measurements for individual scales (taken against a black background of carbon-coated glass) represent three scales in each of three different individuals. The reflectance spectrum for each sample/scale was measured in triplicate at the location marked by a white asterisk in Fig. 1*C* and then averaged. ANOVAs to test for significant differences in mean reflectance between WT and violet scales were calculated for a variety of reflectance points along the spectrum using the JMP statistical software package (v.10, SAS Institute Inc.). The transmittance spectra were taken from individual scales placed on transparent substrates. All reflectance and transmittance spectra were subject to normalization against the Xenon arc lamp emission spectrum. The absorbance spectra were obtained by $-\log_{10}[T'(\lambda)]$, where $T'(\lambda)$ represents the measured transmittance of scales immersed in fluid matching the refractive index.

Scanning Electron Microscopy. Butterfly wings were soaked in a mixture of water and alcohol and then were dipped into liquid nitrogen for ∼5min to ensure thorough freezing. After freezing, the wings were removed from liquid nitrogen and immediately sectioned in the region of the color band using a microtome blade (1). After complete evaporation of the remaining liquid at room temperature, the wing fragment was pressed gently against a conductive carbon tape to transfer the scales onto the tape, which was then attached to the sample mount. The samples were imaged first with an optical microscope to identify the scale type and the color-producing regions on the scales; then they were coated with a layer of gold (∼10 nm) to increase sample conductivity. To obtain cross-sectional scanning electron microscopy images of the scales, the samples were mounted on a rotation stage. All scanning electron microscope images were taken using a SU-70 UHR Schottky (Analytical) FE-SEM (Hitachi High Technologies America, Inc.) at 2 kV accelerating voltage and 28 μA probe current.

Numerical Simulations of Reflectance Spectra from Lower Lamina. A standard thin-film interference model considering multiple reflections within a dielectric film was used to calculate reflectance spectra from the lower lamina of wing scales (2). In our simulation, the medium above and below the dielectric layer is air. We used the wavelength-dependent refractive index (n) of chitin from ref. 3: $n(\lambda) = A + B/\lambda^2$, $A = 1.517$ and $B = 8.80 \times 10^3$ nm^2. In the calculation we also took into account the variation in lower lamina thickness and the range of incident angle of the light in our measurement. Reflectance spectra were computed first for different values of film thickness and incident angle of light. The reflectance spectrum calculated for each incident angle was weighted by the corresponding solid angle to simulate the measured spectrum for one value of lamina thickness. The spectra for the different lamina thicknesses then were averaged by taking a uniform thickness distribution centered at the population mean and with a width equal to the 95% confidence interval. The angle averaging and the thickness averaging reduced the spectral modulation of the reflectance, and the angle averaging also shifted the reflectance peak to a shorter wavelength.

1. Bozzola JJ, Russell LD (1999) Electron Microscopy: Principles and Techniques for Biologists. (Jones and Bartlett, Boston), 2nd Ed.
2. Kinoshita S, Yoshioka S, Miyazaki J (2008) Physics of structural colors. *Rep Prog Phys* 71(7):1–30.
3. Leertouwer HL, Wilts BD, Stavenga DG (2011) Refractive index and dispersion of butterfly chitin and bird keratin measured by polarizing interference microscopy. *Opt Express* 19(24):24061–24066.

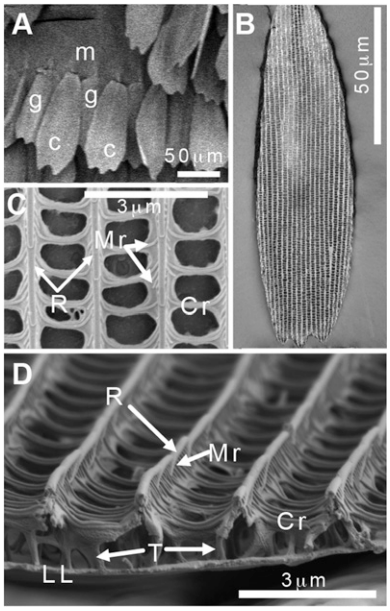

Fig. S1. Scanning electron microscope images of *Bicyclus anynana* brown wing scales showing basic wing morphology. (*A*) Section of the wing where the scales in the top left corner have been removed and the wing membrane (m) is visible. Attached to the membrane are the cover (c) and ground (g) scales, which alternate each other along rows. (*B*) A cover scale showing its fine sculpting on the abwing surface. (*C* and *D*) Top view and tilt view of a *B. anynana* WT cover scale, showing the trabeculae (T) connecting the lower lamina (LL) to the upper lamina, which includes ridges (R), microribs (Mr), and crossribs (Cr).

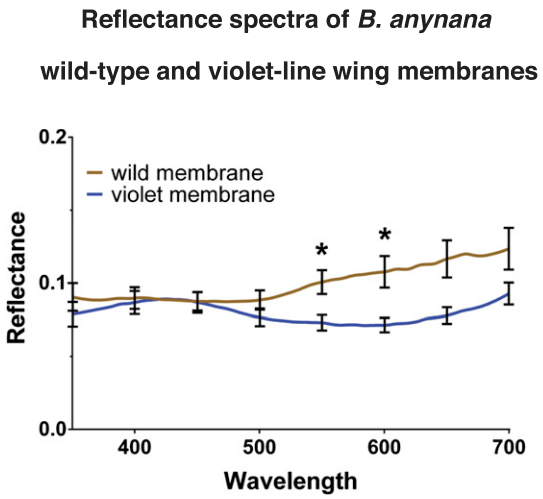

Fig. S2. Mean reflectance spectra of *B. anynana* WT and violet-line wing membranes with all scales removed. Error bars represent standard error of the mean (SEM). Data are the mean of spectra measured in five WT and five violet females. Asterisks represent significant differences between lines.

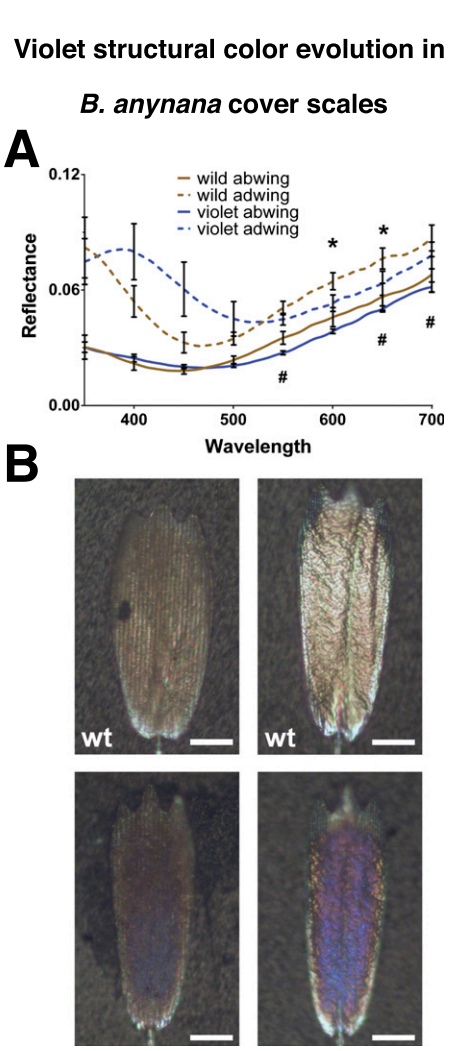

Fig. S3. Evolution of violet structural color in *B. anynana* cover scales. (*A*) Reflectance spectra of the abwing and adwing surfaces of individual cover scale from WT and violet-line individuals. Error bars represent SEM. Asterisks indicate statistically significant differences in reflectance for the adwing surfaces of scales. Pound symbols (#) indicate statistically significant differences in reflectance for abwing scale surfaces (Table S1). (*B*) Images of abwing (*Left*) and adwing (*Right*) surfaces of individual cover scales from WT (*Upper Row*) and violet-line (*Lower Row*) females. (Scale bars: 20 μm.)

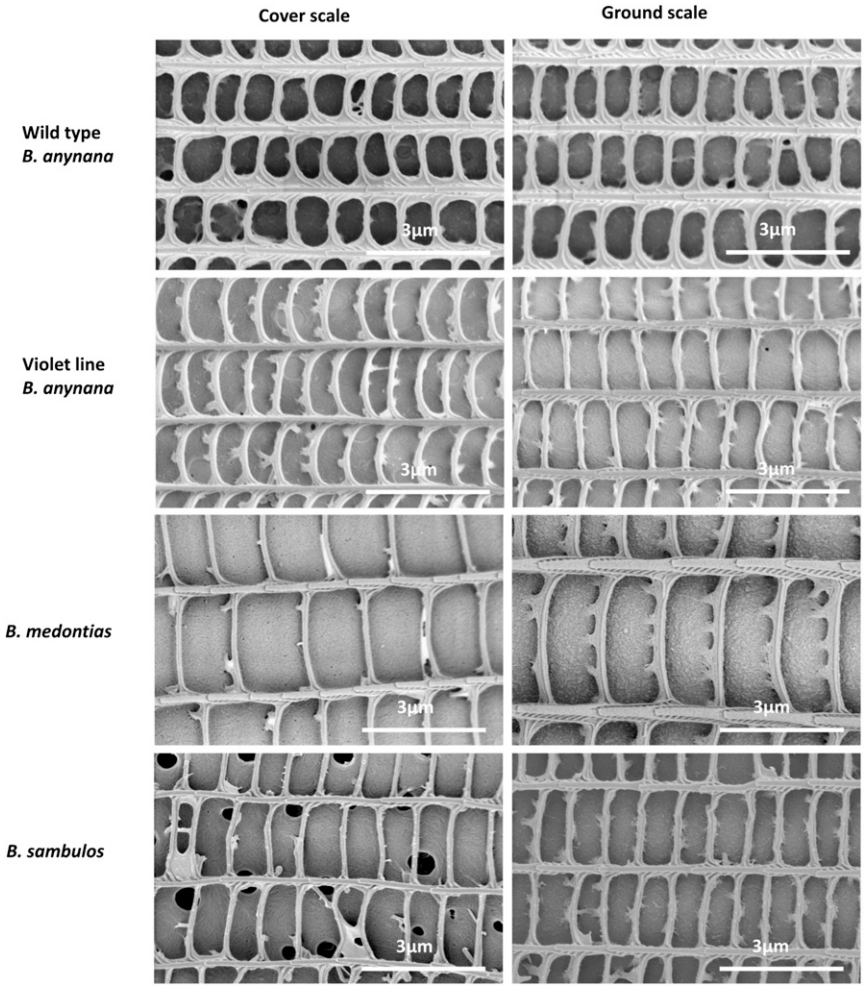

Fig. S4. Top-view scanning electron microscope image**s of** cover (*Left*) and ground (*Right*) scales of WT and violet-line *B. anynana* and violet/blue scales in *Bicyclus sambulos* and *Bicyclus medontias*. The scale structures are similar, and the lower lamina is clearly visible through the windows of the upper lamina.

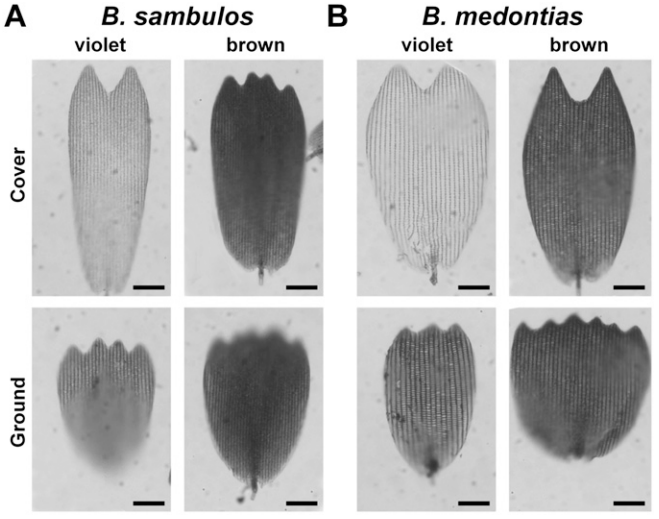

Fig. S5. Transmission of light in *B. sambulos* and *B. medontias* scales. In all transmission images, cover scales are depicted in the upper row, and ground scales are depicted in the lower row. (*A*) *B. sambulos* violet/blue and brown scales. (*B*) *B. medontias* violet and brown scales. (Scale bars: 20 μm.)

Table S1. Comparison of reflectance and absorbance values for the targeted wing area and for individual scales of *B. anynana* WT and violet-line females (generation 8) at wavelengths between 350 and 700 nm

λ, nm	WT	Violet-line	F	*P* value	WT	Violet-line	F	*P* value
	Reflectance on the wing (~1 mm^2)				Reflectance on the individual cover scales on the wing			
350	0.14	0.19	4.67	0.0968	0.15	0.12	1.85	0.1851
400	0.11	0.20	22.83	0.0088*	0.10	0.09	0.17	0.6814
450	0.10	0.18	23.06	0.0086*	0.11	0.08	3.63	0.0672
500	0.13	0.17	11.89	0.0261*	0.16	0.09	10.45	0.0031*
550	0.19	0.19	0.00	0.9534	0.23	0.14	11.25	0.0023*
600	0.25	0.22	3.97	0.1170	0.32	0.19	10.33	0.0033*
650	0.33	0.29	6.11	0.0688	0.39	0.27	2.16	0.1802
700	0.43	0.39	3.03	0.1566	0.44	0.34	1.39	0.2717
	Reflectance on the individual ground scales on the wing				Reflectance on the wing membrane (scales removed)			
350	0.29	0.26	0.50	0.4861	0.48	0.39	1.92	0.1770
400	0.27	0.34	3.79	0.0618	0.45	0.44	0.07	0.7951
450	0.25	0.32	6.61	0.0158*	0.44	0.44	0.01	0.9139
500	0.28	0.28	0.00	0.9935	0.44	0.38	1.72	0.1998
550	0.37	0.31	7.50	0.0106*	0.49	0.37	7.13	0.0125*
600	0.47	0.36	16.59	0.0003*	0.54	0.36	8.94	0.0058*
650	0.56	0.44	11.83	0.0088*	0.59	0.40	3.00	0.1215
700	0.61	0.53	3.43	0.1012	0.60	0.46	1.62	0.2395
	Reflectance on the individual cover scales - abwing				Reflectance on the individual cover scales - adwing			
350	0.16	0.18	0.43	0.5232	0.41	0.46	0.19	0.6698
400	0.11	0.12	0.57	0.4609	0.26	0.39	2.51	0.1328
450	0.09	0.10	1.30	0.2707	0.17	0.31	3.61	0.0756
500	0.12	0.10	1.45	0.2463	0.17	0.22	1.13	0.3027
550	0.18	0.14	4.70	0.0457*	0.26	0.22	1.67	0.2149
600	0.23	0.19	3.14	0.0955	0.32	0.27	4.88	0.0421*
650	0.27	0.24	15.58	0.0169*	0.36	0.31	31.25	0.005*
700	0.32	0.27	14.35	0.0193*	0.40	0.39	0.12	0.7507
	Reflectance on the individual ground scales - abwing				Reflectance on the individual ground scales - adwing			
350	0.27	0.29	0.19	0.6652	0.37	0.38	0.03	0.8557
400	0.19	0.28	5.23	0.0362*	0.27	0.44	6.62	0.0204*
450	0.15	0.23	5.78	0.0287*	0.20	0.37	14.29	0.0016*
500	0.15	0.18	1.66	0.2160	0.16	0.23	5.88	0.0275*
550	0.20	0.17	2.20	0.1571	0.19	0.18	0.17	0.6818
600	0.27	0.20	8.25	0.0111*	0.25	0.19	1.42	0.2513
650	0.34	0.26	30.92	0.0051*	0.31	0.27	1.82	0.2485
700	0.41	0.34	6.60	0.0621	0.38	0.35	0.69	0.4520
	Absorbance individual cover scales				Absorbance individual ground scales			
350	0.21	0.16	2.47	0.1909	0.19	0.13	3.17	0.1496
400	0.26	0.21	1.66	0.2670	0.21	0.16	2.47	0.1911
450	0.25	0.20	1.13	0.3477	0.19	0.14	2.14	0.2171
500	0.22	0.17	1.22	0.3313	0.17	0.11	3.46	0.1366
550	0.20	0.16	0.98	0.3789	0.16	0.09	6.17	0.0679
600	0.17	0.14	0.63	0.4710	0.15	0.07	9.39	0.0375*
650	0.14	0.11	0.49	0.5228	0.13	0.06	10.13	0.0334*
700	0.11	0.09	0.54	0.5040	0.12	0.05	10.09	0.0337*

Measurements on individual scales were done both to scales attached to (reflectance) and removed (reflectance and absorbance) from the wing. ANOVA was used to test for significant differences in mean reflectance or absorbance between WT and violet lines. F statistics and associated *P* values are reported.

*$P < 0.05$.